

Laser Induced Raman Spectra of Some Tungstates and Molybdates*

R. K. Khanna,** W. S. Brower, B. R. Guscott,** and E. R. Lippincott**

Institute for Materials Research, National Bureau of Standards, Washington, D.C. 20234

(August 3, 1967)

The Raman spectra of single crystals of CaWO_4 , CaMoO_4 , PbWO_4 , and PbMoO_4 have been recorded using a He–Ne laser ($\lambda = 6328 \text{ \AA}$) and an Argon ion laser ($\lambda = 4880 \text{ \AA}$) as the exciting radiation sources. The polarization data have enabled us to classify unambiguously the observed fundamentals into the Raman active species of the point group C_{4h} to which these crystals belong. The comparison of the spectra of these crystals in the low frequency region has also enabled us to make a rough classification of the bands into the rotational and the translational lattice vibrations.

Key Words: Molybdates, Raman spectra, tungstates.

1. Introduction

The tungstates and molybdates of the alkaline earths present rather simple cases for correlation of their Raman spectra with the crystal structure. With the availability of high-powered monochromatic laser radiation the Raman spectra of properly oriented single crystals can enable an unambiguous classification of the vibrational modes into the respective species of the point group to which these crystals belong.

The Raman spectrum of CaWO_4 has been reported by Russell and Loudon [1].¹ The authors have been able to identify 11 of the 13 expected long wavelength fundamentals. A comparison with the spectra of PbWO_4 as well as the molybdates of calcium and lead was considered desirable in an effort to get detailed information on the nature of the vibrational modes and to attempt to identify the two missing vibrations of CaWO_4 . The results of the analysis of these spectra form the basis of this report.

2. Experimental Procedure

The tungstate and molybdate crystals were grown by the Czochralski method. They were then oriented by means of the Laue back reflection x-ray method.

subsequently cut and polished to the shape of cubes with the edges coinciding with the major crystallographic axes.

The Raman spectra were recorded on a Cary 81 spectrophotometer equipped with a Helium-Neon Laser ($\lambda = 6328 \text{ \AA}$)² with the incident light perpendicular to the (010) and (001) faces (i.e., along b and c directions). One of the crystallographic axes was made to coincide with the direction of polarization of the incident beam and the scattered light with the components \parallel and \perp to the direction of the incident polarization was recorded.

Since the x and y crystallographic directions are equivalent (as will be elaborated upon in the next section) some of the orientations gave identical spectra. The four independent traces for PbWO_4 are reproduced in figure 1 (a-d). The corresponding traces for PbMoO_4 are produced in figure 2 (a-d).

3. Discussion

The tungstates and molybdates of calcium and lead belong to the well-known scheelite structure (space group $^{14}4_{1/a}-C_{4h}^6$) [2, 3, 4]. The cell of the body-centered tetragonal lattice contains 4 molecules. Since the molecules at the body center are related to those at the corners by simple translations the number of independent vibrational modes of the lattice correspond to those of only two molecules. The usual group theoretical analysis [5] gives the distribution of the vibrations into the irreducible representations of the point group C_{4h} as follows

$$\Gamma = 3A_g + 5B_g + 5E_g + 4A_u + 3B_u + 4E_u.$$

*The work carried out at the University of Maryland has been supported in part by the Advanced Research Projects Agency and a grant from the U.S. Army Research Office, Durham, N.C. For the crystal growth work at the National Bureau of Standards the authors gratefully acknowledge support from the U.S. Atomic Energy Commission.

**Address: Department of Chemistry, University of Maryland, College Park, Md. 20740.

¹ Figures in brackets indicate the literature references at the end of this paper.

² Essentially similar results and much stronger Raman bands were obtained with the argon ion laser ($\lambda = 4880 \text{ \AA}$).

The species with the subscript g are infrared inactive and those with the subscript u are Raman inactive. The 13 Raman active vibrations may be classified into two categories, namely, the internal modes of the XO_4^- ($\text{X} = \text{W}$ or Mo) units and the lattice modes involving the motion of the rigid units. Even though such a classification is convenient, it should be borne in mind that some of the internal modes (particularly the bending modes) may be in strong interaction with some of the lattice modes.

The tetrahedral XO_4^- units occupy S_4 sites in the lattice. The correlation diagram below [5] gives the site as well as the factor group splitting of the internal modes. The last column in the table gives the proper combinations of the polarizability components for the Raman active species for the group C_{4h} .

Figures 1a and b give the Raman spectra of PbWO_4 with the incident radiation along the y -direction with the electric vector \parallel to the z axis and the scattered light collected with the vibration directions of the analyser \parallel and \perp to the z axis respectively. These two traces show, therefore, the vibrations for which α_{zz} and α_{xy} (respectively) are nonzero. Similarly, the spectra reproduced in figure 1c and d, shows the vibrations for which α_{xx} (or α_{yy}) and α_{xy} (respectively) are nonzero. With these basic theoretical results in mind, the interpretation of the spectra becomes fairly straight-forward.

TABLE 1. Site and factor group splittings of the vibrational modes of the XO_4^- ions in the scheelite structure

	T_d	S_4	C_{4h}	
X-O Sym. st.	$\nu_1(A_1)$	A	A_g	$\alpha_{xx} + \alpha_{yy}, \alpha_{zz}$
XO_4^- deg. bend	$\nu_2(E)$	B	B_g, B_u	$\alpha_{xx} - \alpha_{yy}, \alpha_{xy}$
X-O asym. bend	$\nu_3(F_2)$	E	E_g	α_{xz}, α_{yz}
XO_4^- asym. bend	$\nu_4(F_2)$		E_u	

Thus, the band at $\sim 900 \text{ cm}^{-1}$ for which α_{zz} , α_{xx} and α_{yy} are nonzero is associated with the $\nu_1(A_g)$ mode. The bands at $\sim 764 \text{ cm}^{-1}$ and at $\sim 748 \text{ cm}^{-1}$ which have the characteristics B_g and E_g respectively, appear to be the 2 split components of the $\nu_3(F_2)$ mode of the XO_4^- ion. The corresponding bending mode $\nu_4(F_2)$ also shows 2 components [353 cm^{-1} (E_g) and 348 cm^{-1} (B_g)]. A relatively smaller splitting of $\nu_4(F_2)$ compared to that of $\nu_3(F_2)$ is quite general for the tetrahedral ions and has received an explanation by Greenwood [6]. In this connection mention may be made of the observation of only one component of ν_4 in the spectrum of CaWO_4 reported by Russell and Loudon. Our traces for CaWO_4 show two components for ν_4 [403 cm^{-1} (B_g) and 397 cm^{-1} (E_g)]. The doubly degenerate mode $\nu_2(E)$ should also be split in the lattice. The band is rather broad and appears with components α_{zz} , α_{xx} , α_{yy} , and α_{xy} . Apparently, the small splitting, if any, is lost in the band width. The internal modes of PbMoO_4 , CaWO_4 and CaMoO_4 also show very similar results. The assignments of the observed bands in all the spectra are given in table 2.

TABLE 2. Assignments of the fundamental vibrational modes of AXO_4 , $\text{A} = \text{Ca}, \text{Pb}$; $\text{X} = \text{W}, \text{Mo}$
(Designated by wave numbers in cm^{-1})

	CaWO_4	PbWO_4	CaMoO_4	PbMoO_4	
Russell & Loudon					
86 (B_g)	86 (B_g) 86 (E_g) ?	76 (B_g) 61 (E_g) 52 (B_g) 86 (E_g)	111 (B_g) 111 (E_g) ?	75 (B_g) 61 (E_g) 64 (B_g) 100 (E_g)	$A^{++} - A^{++}(\text{st}) z$ $A^{+-} - A^{++}(\text{st}) xy$ $\text{XO}_4^{--} - \text{XO}_4^{--}(\text{st}) z$ $\text{XO}_4^{--} - \text{XO}_4^{--}(\text{st}) xy$
118 (E_g) 180 ?	116 (E_g)	187 (E_g)	140 (E_g)		
196 (E_g) 210 (A_g) 281 (E_g)	196 (E_g) 210 (A_g)	187 (E_g) 178 (A_g)	189 (E_g) 204 (A_g)	190 (E_g) 164 (A_g)	R_{xy} R_z
334 (A_g)	333 (A_g)	322 (A_g)	322 (A_g)	314 (A_g)	
	333 (B_g) 397 (B_g)	322 (B_g) 348 (B_g)	322 (B_g) 390 (B_g)	317 (B_g) 348 (B_g)	ν_2
403 (B_g)	403 (E_g) 403 (E_g)	348 (B_g) 353 (E_g)	390 (B_g) 404 (E_g)	348 (B_g) 356 (E_g)	ν_4
794 (E_g)	795 (E_g)	748 (E_g)	794 (E_g)	744 (E_g)	ν_3
838 (B_g)	838 (B_g)	764 (B_g)	844 (B_g)	764 (B_g)	ν_1
922 (A_g)	911 (A_g)	900 (A_g)	878 (A_g)	868 (A_g)	

The bands below 300 cm^{-1} are predominantly due to lattice modes and their assignments to the various species follow the same arguments as for the internal modes. PbWO_4 and PbMoO_4 show six bands with the predicted polarization characteristics for the fundamentals. CaWO_4 and CaMoO_4 show fewer bands. A comparison of the spectra of the four crystals and a rough description of the lattice modes might enable us to locate the missing modes in the latter two crystals. The lattice modes belong to the following irreducible representations of the group C_{4h} .

$$\Gamma = A_g + 2B_g + 3E_g.$$

The mode A_g involves torsional motion (R_2) of the XO_4^- about the z axis and the torsional motion about the two orthogonal axes (R_x and R_y) in the x - y plane have the E_g characteristics.

The assignment R_z ($\sim 178 \text{ cm}^{-1}$ in PbWO_4 and 164 cm^{-1} in PbMoO_4) is quite unambiguous as this is the only band possessing nonzero α_{xx} , α_{yy} , and α_{zz} components. For the most favorable arrangement in a cubic lattice R_x , R_y , and R_z would coincide. Consequently, the band adjacent to R_z ($\sim 187 \text{ cm}^{-1}$) having nonzero α_{xz} and α_{yz} components is assigned to R_x and R_y (E_g). The bands at 61 cm^{-1} (E_g) and 76 cm^{-1} (B_g) in the spectrum of PbWO_4 have almost exact counterparts in that of PbMoO_4 and, therefore, are assigned to Pb-Pb stretches in the x - y plane (E_g) and along the z axis (B_g) respectively. The remaining two bands, namely 52 cm^{-1} (B_g) and 86 cm^{-1} (E_g) in the spectrum of PbWO_4 [64 cm^{-1} (B_g) and 86 cm^{-1} (E_g) in PbMoO_4] may be assigned to the translatory lattice modes involving motions of the XO_4^- units.

Only four of the six lattice modes of CaWO_4 and CaMoO_4 can be assigned with certainty (table 2). However, an examination of the spectra reveals that the band at $\sim 86 \text{ cm}^{-1}$ in CaWO_4 ($\sim 110 \text{ cm}^{-1}$ in CaMoO_4) have both B_g and E_g polarizations. It is quite likely that the modes involving translations of Ca^{++} along the z axis and in the x - y plane still retain their degeneracy. The other missing mode (presumably involving translation of the XO_4^- units along the z direction) is presumably too weak. Russell and Loudon

have reported two weak bands, one at $\sim 180 \text{ cm}^{-1}$ with unspecified polarization and the other at $\sim 281 \text{ cm}^{-1} (E_g)$ in the spectrum of CaWO_4 . Our records also show these two bands, but the former appears in all orientations and the latter is rather broad, and may be due to the second order processes.

By a detailed analysis of the Raman scattering in calcite, Porto et al. [7], have concluded that the polarization errors can be quite large if the incident (convergent) or the scattered light travels along the optic axis of a uniaxial crystal. For a ray diverging as little as 1° from the optic axis the depolarization is

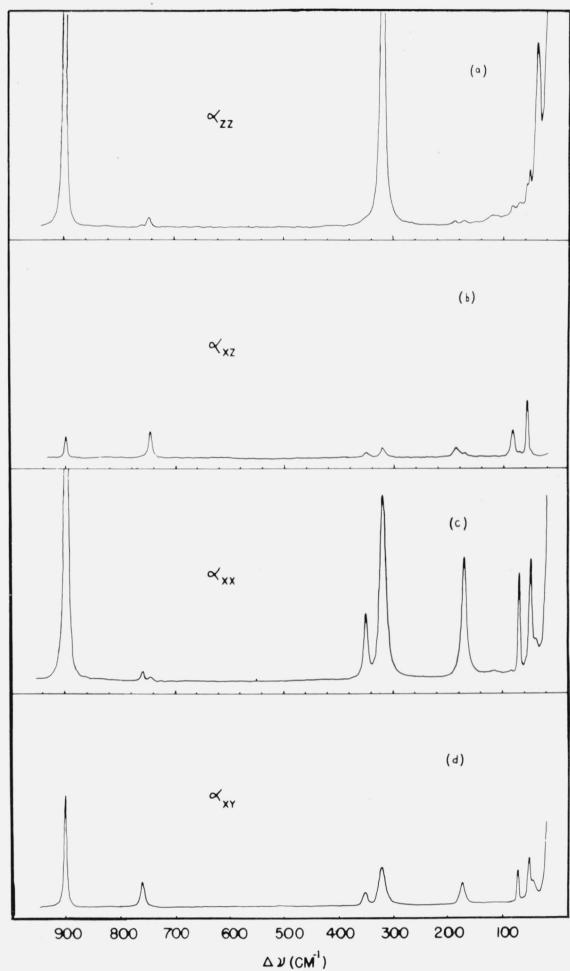


FIGURE 1. Raman spectrum of PbWO_4 , spectral slit width $\sim 3 \text{ cm}^{-1}$.

- (a) α_{zz} component showing A_g vibrations
 (b) α_{xz} ($=\alpha_{yz}$) component showing E_g vibrations
 (c) α_{xx} component showing A_g and B_g vibrations
 (d) α_{xy} component showing B_g vibrations.

Weak residual components of A_g and B_g in (b) are due to convergence of the scattered beam.

Finally, a remark on the traces in figure 1d and figure 2d is called for. It is seen that the band at $\sim 900 \text{ cm}^{-1} [\nu_1(A_{1g})]$ appears with an appreciable intensity with α_{xy} polarization in apparent contradiction with the selection rules. A similar anomaly in the $\nu_1(A_{1g})$ band of calcite ($\sim 1086 \text{ cm}^{-1}$) has been noted in the past and its explanation in terms of unspecified convergence error has been attempted.³

³ See reference 7 and the cross references indicated there.

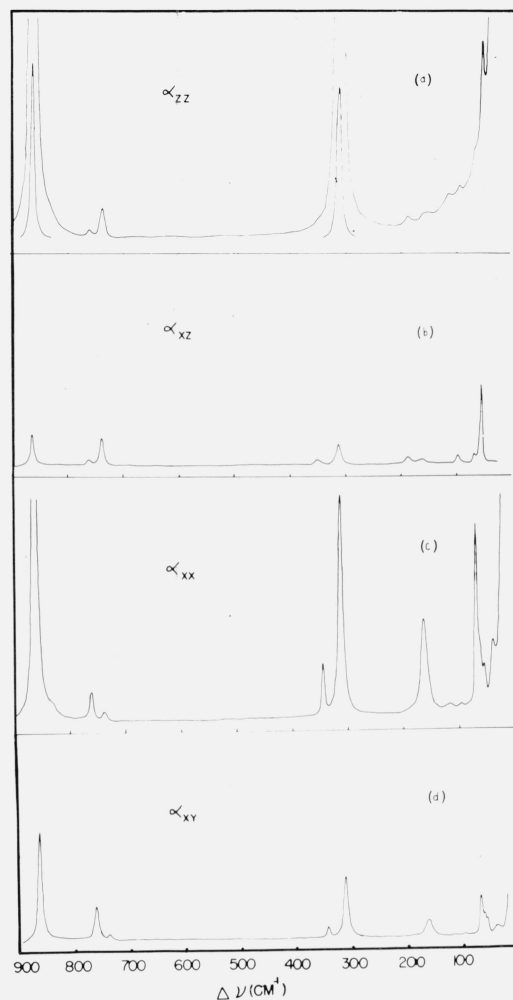


FIGURE 2. Raman spectrum of PbMoO_4 .

Captions in the figure have the same meaning as in figure 1.

more or less complete after the beam traverses a path length of $\sim 5 \text{ mm}$. The spectra reported in figure 1d and figure 2d were recorded with the incident light along the z axis (optic axis) from a focused laser beam with x polarization and the scattered light with the y component was collected within a cone of an estimated 6° half angle, thereby giving a finite intensity to the A_g bands.

The authors are indebted to E. N. Farabaugh for the x-ray orientation of the crystals used in this study and to H. S. Peiser for encouragement and helpful discussions.

4. References

- [1] J. P. Russell and R. Loudon, Proc. Phys. Soc. London **85**, 1029 (1965).
- [2] R. D. Burbank, Acta Cryst. **18**, 88 (1965).
- [3] A. Zalkin and T. H. Templeton, J. Chem. Phys. **40**, 501 (1964).
- [4] B. C. Frazer and I. Almodoran, J. Chem. Phys. **40**, 504 (1964).
- [5] E. B. Wilson, J. C. Decius and P. C. Cross, Molecular Vibrations (McGraw-Hill Book Co., New York, N.Y., 1955).
- [6] N. N. Greenwood, J. Chem. Soc., 3811 (1959).
- [7] S. P. S. Porto, J. A. Giordmaine and T. C. Damen, Phys. Rev. **147**, 608 (1966).

(Paper 72A1-483)